

Hallucination Detection in LLMs via Topological Divergence on Attention Graphs

Alexandra Bazarova¹ Aleksandr Yugay¹ Andrey Shulga¹ Alina Ermilova¹ Andrei Volodichev¹
 Konstantin Polev² Julia Belikova² Rauf Parchiev² Dmitry Simakov² Maxim Savchenko²
 Andrey Savchenko² Serguei Barannikov^{1,3} Alexey Zaytsev¹

Abstract

Hallucination, i.e., generating factually incorrect content, remains a critical challenge for large language models (LLMs). We introduce TOHA, a TOPology-based HALLucination detector in the RAG setting, which leverages a topological divergence metric to quantify the structural properties of graphs induced by attention matrices. Examining the topological divergence between prompt and response subgraphs reveals consistent patterns: higher divergence values in specific attention heads correlate with hallucinated outputs, independent of the dataset. Extensive experiments — including evaluation on question answering and data-to-text tasks — show that our approach achieves state-of-the-art or competitive results on several benchmarks, two of which were annotated by us and are being publicly released to facilitate further research. Beyond its strong in-domain performance, TOHA maintains remarkable domain transferability across multiple open-source LLMs. Our findings suggest that analyzing the topological structure of attention matrices can serve as an efficient and robust indicator of factual reliability in LLMs.

1. Introduction

Large language models (LLMs) have progressed significantly in recent years, finding applications in various fields (Chkirbene et al., 2024). However, these models are prone to generate so-called *hallucinations*, i.e., content that is factually or contextually incorrect (Huang et al., 2023). Detecting hallucinations is crucial for the safe deployment of LLMs in sensitive fields since erroneous outputs may lead to financial losses and seriously harm user trust.

¹Skolkovo Institute of Science and Technology ²Sber AI Lab
³CNRS, Université Paris Cité. Correspondence to: Alexandra Bazarova <a.bazarova@skoltech.ru>.

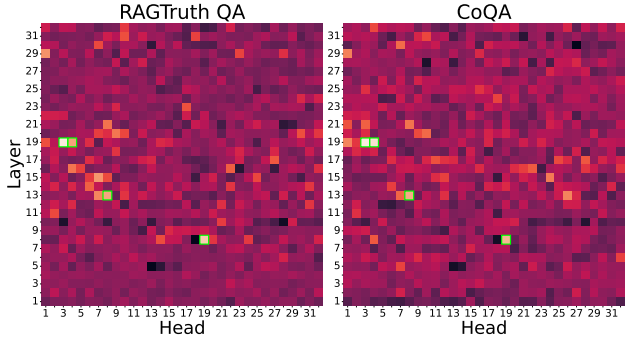


Figure 1. Difference between average TOHA scores for hallucinated and grounded samples per attention head/layer, evaluated on RAGTruth QA and CoQA datasets. A lighter color corresponds to a greater difference. Green frames highlight the heads that segregate samples best. The same attention heads assign greater divergence values to the hallucinated samples in both datasets. Model: Mistral-7B-Instruct-v0.1.

Both supervised and unsupervised methods address this issue (Azaria & Mitchell, 2023; Fadeeva et al., 2024). Despite the high accuracy of supervised methods, they are often poorly transferable between different datasets and tasks (Sky et al., 2024). Additionally, there are very few natural hallucination datasets publicly available (Zhang et al., 2023); therefore, time-consuming and expensive annotation work is necessary to attain real-life hallucination classifiers. Unsupervised methods, though not suffering from these issues, tend to be computationally intensive, as their inference often includes generating multiple model outputs (Manakul et al., 2024; Chen et al., 2024; Farquhar et al., 2024).

We address the above challenges by introducing TOHA, a novel training-free method to detect LLMs’ hallucinations in the retrieval-augmented generation (RAG) setting (Gao et al., 2023). TOHA focuses on attention maps in LLMs based on the hypothesis that their structure may reflect the presence of hallucinations. Since the graph representation of attention maps has proven effective for various NLP tasks (Kushnareva et al., 2021; Tulchinskii et al., 2023), TOHA also employs it to obtain hallucination scores. The

previous works (Proskurina et al., 2023a; Cherniavskii et al., 2022) have analyzed attention graphs rather naively by building a simple supervised classifier on top of graph properties; our experiments (see Appendix D) reveal that this applying this approach to hallucination detection falls short of achieving the desired accuracy.

TOHA takes the next step in developing a more advanced graph analysis tool. We assume that the presence of hallucinations in the RAG setting may be indicated by the topological dissimilarity of the response subgraph concerning the prompt one. Simply put, a hallucinated response likely includes information that is not present in the prompt, which introduces its unique structure to the text. As a result, we expect the topology of hallucinated responses to differ from that of grounded ones. We draw an analogy between the considered idea of measuring the dissimilarity between two subgraphs and the Manifold Topology Divergence (Baranikov et al., 2021) and then propose its counterpart in the graph setting. For the latter, we prove several properties regarding its continuity and boundedness to ensure it can be considered a reasonable hallucination score.

Our contributions are the following:

- We propose TOHA, a training-free method based on the topological divergences of attention graphs. TOHA demonstrates strong in-domain performance and maintains domain transferability across different tasks. Our method offers an efficient and practical solution, working an order of magnitude faster than unsupervised methods of comparable performance.
- The existence of hallucination-aware attention heads is discovered: calculating topological divergences from just a few specific heads is enough for reliable hallucination detection, irrespective of the dataset.
- We release two novel datasets containing outputs from several popular open LLMs, annotated for hallucination, to facilitate benchmarking and further research in the field.
- For all considered benchmarks, TOHA demonstrates competitive results in the unsupervised and transfer settings for several open-sourced LLMs, including LLaMA-2-13B.

2. Related works

Hallucination detection methods. The problem of hallucinations in LLMs has attracted significant attention, leading to the development of methods for their detection (Zhang et al., 2023; Huang et al., 2023; Wang et al., 2024). Several approaches leverage a model’s internal states to detect hallucinations in a supervised manner. For instance, (Azaria

& Mitchell, 2023; Sky et al., 2024) demonstrated that classifiers trained on hidden states effectively identify factual errors. In contrast, (Chuang et al., 2024) introduced look-back ratio features from attention weights to train a linear classifier for hallucination detection. However, supervised methods depend on annotated datasets, which are costly to create and may not generalize well across diverse tasks (Sky et al., 2024). Unsupervised approaches instead exploit a model’s uncertainty, using token or sequence probabilities to estimate confidence during generation (Kadavath et al., 2022; Fadeeva et al., 2024). Another line of work analyzes inconsistencies across multiple responses to the same input. For example, the INSIDE method (Chen et al., 2024) quantifies hallucinations by measuring differential entropy in the embedding space, while semantic entropy (Han et al., 2024; Farquhar et al., 2024) assesses uncertainty by computing entropy over clusters of semantically similar responses. For black-box models, where internal states and token probabilities are inaccessible, textual analysis methods have been developed (Manakul et al., 2024; Xiong et al., 2024). While considering multiple generations of responses can provide valuable insights for hallucination detection, it increases computational costs significantly and may not scale efficiently for real-time applications.

Evaluation. Hallucination detection methods are typically evaluated in tasks such as summarization (Narayan et al., 2018), open-ended text generation (Lebret et al., 2016), and question answering (Rajpurkar et al., 2016). In structured settings, such as multiple-choice questions in TruthfulQA (Lin et al., 2022) or True/False statements (Azaria & Mitchell, 2023), automatic methods allow for direct comparison with reference answers and the computation of classification metrics. In contrast, hallucinations in open-ended responses are usually annotated by human experts, as seen in FELM (Zhao et al., 2023) and RAGTruth (Niu et al., 2023). Since this process is costly and time-consuming, recent studies have leveraged LLMs to generate annotations (Lin et al., 2022; Min et al., 2023), demonstrating strong agreement with human judgments. Despite these advances, most publicly available datasets provide hallucination annotations for black-box models such as GPT-3 (Brown et al., 2020), making them unsuitable for studying hallucination detection based on a model’s internal states. To the best of our knowledge, RAGTruth (Niu et al., 2023) is the only dataset that includes annotated outputs from open-source models such as LLaMA (Touvron et al., 2023) and Mistral (Jiang et al., 2023) in the RAG setting.

Topological Data Analysis (TDA) in NLP. Topological Data Analysis is a mathematical framework that analyzes multi-scale intrinsic structural patterns in data using principles from topology and computational geometry (Chazal & Michel, 2017; Hensel et al., 2021). The application of TDA

tools in NLP has gained increasing attention (Uchendu & Le, 2024). For instance, (Tulchinskii et al., 2024) applied the Persistent Homology Dimension estimator of intrinsic dimensionality to CLS embeddings of texts to detect artificially generated content. Other studies have also explored calculating topological features from transformer attention matrices to assess uncertainty (Kostenok et al., 2023) or perform grammatical acceptability classification (Proskurina et al., 2023b). In these studies, attention matrices were treated as weighted graphs, and TDA features of these graphs were employed to train simple classifiers on top of them.

3. Background

3.1. Attention matrix as a weighted graph

Modern LLMs are mainly based on the self-attention mechanism, introduced in (Vaswani et al., 2017). This mechanism enables models to dynamically assign varying levels of importance to different parts of the input sequence when generating the output.

Let $X \in \mathbb{R}^{n \times d}$ be a matrix consisting of d -dimensional representations of n tokens, $W_Q, W_K, W_N \in \mathbb{R}^{d \times d}$ be trainable projection matrices.

Given a set of queries $Q = XW_Q \in \mathbb{R}^{n \times d}$, a set of keys $K = XW_K \in \mathbb{R}^{n \times d}$, and corresponding values $V = XW_V \in \mathbb{R}^{n \times d}$, the attention mechanism calculates a weighted sum of the values as follows:

$$\text{Attention}(Q, K, V) = \text{softmax} \left(\frac{QK^T}{\sqrt{d}} \right) V. \quad (1)$$

Each entry w_{ij} in the attention matrix

$$W = \text{softmax} \left(\frac{QK^T}{\sqrt{d}} \right) \quad (2)$$

captures how strongly token i attends to token j , $i \geq j$ for a decoder, with larger w_{ij} indicating closer relationship.

An attention matrix W can be represented as a complete weighted graph G , whose vertices are the tokens and whose edges carry weights w_{ij} . From the perspective of topological data analysis, however, it is more convenient to interpret these weights as pseudo-distances rather than correlation measures. Hence, we reassign the edge weights of such a graph to be equal to $1 - w_{ij}$. We refer to such graphs as *attention graphs*.

3.2. Manifold Topology Divergence

Given an attention matrix for the (prompt + response) text, we construct the pseudo-distances graph, imitating a data manifold of the text, and study its relation with the weighted subgraph, imitating the data submanifold of the prompt.

Proposed in (Barannikov et al., 2021), $\text{MTop-Div}(M, N)$ is a topological measure for comparing two data manifolds \mathcal{M} and \mathcal{N} approximated by point clouds M and N . This divergence is based on the Cross-Barcode(M, N) tool. Here, we briefly describe these objects; see Appendix A for more details and motivation.

To measure how far the two manifolds \mathcal{M} and \mathcal{N} are from being identical, (Barannikov et al., 2021) considered the independent topological features of the quotient space $\mathcal{M}/(\mathcal{M} \cap \mathcal{N})$. The triviality of this space would entail that natural maps between the homology groups

$$\begin{aligned} \varphi_r : H_*(\mathcal{M} \cap \mathcal{N}) &\rightarrow H_*(\mathcal{M}), \\ \varphi_p : H_*(\mathcal{M} \cap \mathcal{N}) &\rightarrow H_*(\mathcal{N}) \end{aligned} \quad (3)$$

are isomorphisms; simply put, the more trivial $\mathcal{M}/(\mathcal{M} \cap \mathcal{N})$ is, the closer the two manifolds are to being identical. To build the counterpart of this construct for manifolds represented by point clouds, the pair $(\mathcal{M} \cap \mathcal{N}) \subseteq \mathcal{M}$ is replaced with the analogous $\mathcal{N} \subseteq (\mathcal{M} \cup \mathcal{N})$. Taking the quotient is realized by setting the pairwise distances within the point cloud N to zero. Denoting by $m_{(\mathcal{M} \cup \mathcal{N})/N}$ the resulting matrix of pairwise distances, $\text{Cross-Barcode}_i(M, N)$ is the i -th homology barcode (Barannikov, 1994) of the Vietors-Rips simplicial complex $VR_\alpha(M \cup N, m_{(\mathcal{M} \cup \mathcal{N})/N})$. $\text{MTop-Div}(M, N)$, in turn, is the sum of interval lengths of $\text{Cross-Barcode}_i(M, N)$. In the original paper, the authors considered $i = 1$.

4. Method

Let V_X and E_X denote the vertex and edge sets of a graph X , respectively. In the natural language generation process, two subsets of an attention graph G vertex set naturally stand out. The first, P , represents the prompt tokens. The second, $R = V_G \setminus P$, corresponds to the response tokens. An example of an attention graph and corresponding vertex subsets is illustrated in Figure 2b.

To evaluate the probability of hallucination in the RAG setting, we would like to estimate how much of the “independent” knowledge is captured in the response concerning the prompt. Intuitively, when a hallucination occurs, it means that the information in the response was not presented in the prompt. We expect the corresponding vertex set R , along with its edges, to modify the structure of G in an essentially non-trivial way, resulting in the appearance of independent topological features.

Our method relies on the observation that estimating the non-triviality of the response concerning the prompt is analogous to the construction of MTop-Div . Indeed, the resulting $\text{MTop-Div}(M, N)$ measures how non-trivial the topological structure of $M \cup N$ is concerning N . However, MTop-Div was designed for point clouds, and certain of

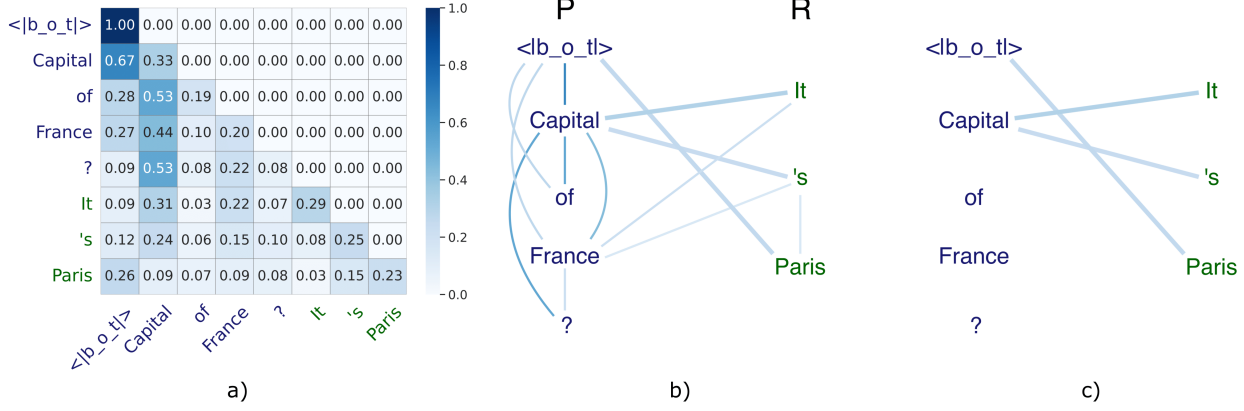


Figure 2. a) An attention map. Blue denotes the prompt tokens, and green is the response ones. b) The corresponding attention graph G . Prompt tokens P are located on the left, response tokens R — on the right. To keep the figure neat, we only plot the edges with an attention score of no less than 0.15. c) The minimum spanning forest attaching R to P .

its properties are based on the fact that M and N lie in \mathbb{R}^n . The structure of our task is different, as the graphs are not metric spaces. We reformulate MTop-Div for the graph context below, establishing its properties in a novel setting.

4.1. MTop-Div for attention graphs

By the analogy formulated above, we develop $\text{MTop-Div}(R, P)$, where R and P are the response and the prompt vertex sets in the attention graph G . Hereinafter, we refer to R and P as *complementary* vertex sets so that the union of these vertex sets and the edges between all these vertices comprises the complete graph G . We next set to zero the edge weights between the P vertices, denote $w_{(R \cup P)/P}$ the resulting matrix of edge weights, define $\text{Cross-Barcode}_i(R, P)$ as the i -th homology barcode of the Vietoris-Rips simplicial complex $VR_\alpha(G, w_{(R \cup P)/P})$, and $\text{MTop-Div}(R, P)$, as the sum of interval lengths of $\text{Cross-Barcode}_i(R, P)$.

Taking into account the specifics of our task, we consider $\text{Cross-Barcode}(R, P)$ for the homology group H_0 instead of H_1 , as the resulting $\text{MTop-Div}(R, P)$ would thus be more interpretable. Indeed, the bars in the H_0 barcode of a weighted graph correspond to edges of the minimum spanning tree (MST) of this graph (Tulchinskii et al., 2023). Similarly, we show that our score equals the length of the minimum spanning forest (MSF) attaching R to P .

Basic properties of MTop-Div for attention graphs. Now we consider specific properties for our adaptation of $\text{MTop-Div}(R, P)$.

Proposition 4.1. *The following holds for any attention graph G and its complementary vertex subsets $P, R \subset V_G$.*

- $\text{MTop-Div}(R, P)$ value equals the length of the MSF attaching R to P .

- Let the natural norm on the cross-barcodes be defined as follows:

$$\|\text{Cross-Barcode}_0\|_B = \max_{[b_j, d_j] \in \text{Cross-Barcode}_0} (d_j - b_j). \quad (4)$$

The norm of $\text{Cross-Barcode}_0(R, P)$ lays in the interval $[0, 1]$:

$$0 \leq \|\text{Cross-Barcode}_0(R, P)\|_B \leq 1. \quad (5)$$

- The divergence itself is bounded by

$$0 \leq \text{MTop-Div}(R, P) \leq |R|. \quad (6)$$

The second and third statements are immediately obtained from the properties of an attention matrix: all its weights lie between 0 and 1.

Proposition 4.2. *Let G be an attention graph, $P, R \subset V_G$ — a pair of complementary vertex subsets.*

1. **(Continuity of MTop-Div(R, P)).** *If the weights of G change by no more than ε , then the corresponding $\text{MTop-Div}(R, P)$ changes by no more than $\delta = \varepsilon|R|$.*
2. **(Exact sequence).** *For any α , the following sequence of natural maps of homology groups is exact*

$$(\mathbb{Z}/2\mathbb{Z})^{|P|} \xrightarrow{r_2} H_0(VR_\alpha(G)) \xrightarrow{r_1} H_0(VR_\alpha(G, w_{(R \cup P)/P})) \xrightarrow{r_0} 0.$$

See proof in Appendix A.

4.2. Universal heads

We hypothesize, inspired by prior investigations in LLM interpretability (Voita et al., 2019; Gould et al., 2024), that particular attention heads exhibit distinct patterns related to hallucinations. To identify such heads, we analyzed head-specific topological divergences as follows.

Denote by h_{ij} the j -th attention head from the layer i . For the specific data sample s and head h_{ij} , let G_{ij}^s be the corresponding attention graph, P_{ij}^s, R_{ij}^s — its prompt and response vertex subsets. Let

$$d_{ij}(s) = \frac{1}{|R_{ij}^s|} \text{MTop-Div}(R_{ij}^s, P_{ij}^s).$$

We examined typical values of this score for different heads and layers. The average distance between hallucinated and grounded examples from the train data for each model’s head is the following:

$$\Delta_{ij} = \frac{1}{|S_{\text{hallu}}|} \sum_{s \in S_{\text{hallu}}} d_{ij}(s) - \frac{1}{|S_{\text{gr}}|} \sum_{s \in S_{\text{gr}}} d_{ij}(s),$$

where S_{hallu} stands for all hallucinated samples from the training set, and S_{gr} stands for all grounded training samples. The obtained differences are displayed in Figure 3 for three datasets.

For each model-dataset pair, we highlighted the top 4 attention heads that demonstrated the highest distance between the divergences of hallucinated and non-hallucinated samples. It can be seen that top heads overlap: for both models, two heads — (19, 3), (8, 19) for Mistral-7B, and (12, 16), (9, 26) for Llama-2-7B — are present across all datasets.

4.3. TOHA

The existence of universal hallucination patterns in the attention heads underlies our method. In this subsection, we present our procedure for hallucination detection TOHA.

Here, we used the notation from the previous paragraph. Our method employs two “probe” sets S_h, S_g containing annotated data to arrange model heads from the most segregating to the least segregating based on Δ_{ij} values, where ij is a head index in a model. During testing, hallucination scores are computed as the average topological divergence values from the top N_{opt} heads, where N_{opt} is a hyperparameter selected on the validation set V . In our experiments, we consider $N_{\text{opt}} \leq N_{\text{max}}, N_{\text{max}} = 6$ to minimize the required amount of computations. The pseudocode for the proposed approach during head selection and inference is presented in Algorithm 1.

5. Experiments

Datasets. In our paper, we used three datasets: RAGTruth (Niu et al., 2023), CoQA (Reddy et al., 2019), and SQuAD (Rajpurkar et al., 2016). The RAGTruth dataset consists of manually annotated responses of several LLMs in the RAG setting. It includes hallucinations in three tasks: question answering (QA), text summarization (Summ), and data-to-text writing (Data2txt). The annotations are word-level; we, in turn, predict response-level labels, considering

Algorithm 1 TOHA algorithm

Require: $d_{ij}(s)$ — divergence between prompt and response for a sample s , S_h, S_g — probe sets; V — validation set of annotated samples $\{(s, y_s)\}_{s \in V}$; T — test set.

procedure TOHA HEADS SELECTION

```

 $\Delta_{ij} \leftarrow \frac{1}{|S_h|} \sum_{s \in S_h} d_{ij}(s) - \frac{1}{|S_g|} \sum_{s \in S_g} d_{ij}(s)$ 
 $H \leftarrow \text{sort}(h_{ij}, \text{key} = \Delta_{ij}, \text{ascending} = \text{False})$ 
 $N, N_{\text{opt}} \leftarrow 1, 1$ 
 $H_{\text{subset}} \leftarrow \emptyset$ 
 $\text{AUROC}_{\text{max}} \leftarrow 0$ 
 $p_s = 0, s \in V$   $\triangleright$  Initialize hallucination scores.
while  $N \leq N_{\text{max}}$  do  $\triangleright$  Optimal heads selection.
     $H_{\text{subset}} \leftarrow H_{\text{subset}} \cup \{h_N\}$ 
    for  $s \in V$  do
         $p_s \leftarrow \frac{N-1}{N} p_s + \frac{1}{N} d_{h_N}(s)$ 
    end for
     $\text{AUROC} \leftarrow \text{AUROC}(\{y_s\}_{s \in V}, \{p_s\}_{s \in V})$ 
    if  $\text{AUROC} > \text{AUROC}_{\text{max}}$  then
         $\text{AUROC}_{\text{max}} \leftarrow \text{AUROC}$ 
         $N_{\text{opt}} \leftarrow N$ 
    end if
     $N \leftarrow N + 1$ 
end while
end procedure

```

procedure TOHA PREDICTION

```

for  $s \in T$  do  $\triangleright$  Prediction on the test set.
     $p_s \leftarrow \frac{1}{N_{\text{opt}}} \sum_{i=1}^{N_{\text{opt}}} d_{h_i}(s)$ 
end for
end procedure

```

a response hallucinated if it contains at least one hallucination span.

CoQA and SQuAD are both question-answering benchmarks. For all the considered models, we used questions from these datasets to sample responses from LLMs and then annotated the responses in an automated manner using GPT-4o (Hurst et al., 2024). We only annotate SQuAD responses for LLaMA-3.1-8B and Qwen2.5-7B due to time and budget limitations.

To estimate the correctness of GPT-4o annotations, we evaluated their consistency with the labels produced by human experts. Our findings indicated that the consistency between the experts and GPT-4o is sufficient to use the latter for annotation, which aligns well with previous works (Bavaresco et al., 2024).

We are contributing by releasing the obtained datasets to the public. Additionally, we provide a straightforward annota-

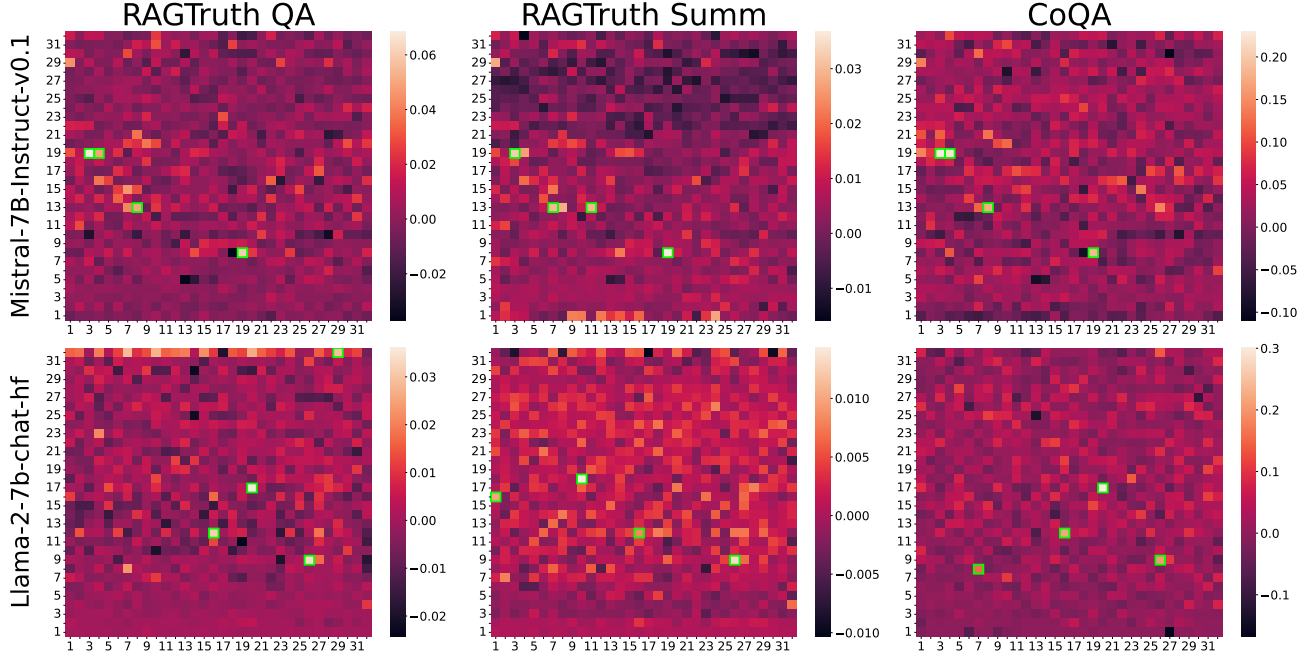


Figure 3. Δ_{ij} values for the datasets RAGTruth QA, RAGTruth Summ, CoQA. A lighter color corresponds to a greater value. Vertical axis corresponds to the layer number, horizontal — to the head number. The heads that segregate samples best are highlighted with green frames. Model names for a row are on the left side.

tion procedure to support further research on hallucination detection. For more details, see Appendix C.

Models. We used five popular open-source LLMs: LLaMA-2-7B-chat, LLaMA-2-13B-chat, LLaMA-3.1-8B-Instruct, Mistral-7B-Instruct-v0.1, and Qwen2.5-7B-Instruct. Note that the RAGTruth dataset does not contain responses for LLaMA-3.1-8B and Qwen-2.5-7B; therefore, we only conducted experiments on SQuAD and CoQA for these models.

Baselines. We compare TOHA with six baselines, including two supervised methods, such as linear probe and attention-pooling probe (Sky et al., 2024), and four unsupervised methods: tokenwise entropy (Fadeeva et al., 2024), semantic entropy (Farquhar et al., 2024), INSIDE (Chen et al., 2024), and SelfCheckGPT (Manakul et al., 2024). Appendix E provides information on implementation details.

Hallucination detection results. Tables 1–2 demonstrate the results of our experiments. As probe and validation datasets for TOHA, we used the training subset of the RAGTruth QA benchmark, split into three parts. All methods were evaluated on the same fixed test set for each dataset. Table 2 contains only two datasets since, as we mentioned, the RAGTruth dataset does not contain annotated samples for this model.

As anticipated, supervised methods outperform unsupervised ones, achieving the ROC-AUC score close to 1 on the SQuAD and CoQA datasets. Most importantly, we would like to highlight the performance of TOHA, which stands out among unsupervised approaches. It consistently achieves the best or second-best results across multiple datasets. Its main competitor in the unsupervised category is SelfCheckGPT. However, it is worth noting that SelfCheckGPT relies on additional model generations (following the original paper, we used 20 in our experiments), making it computationally inefficient. At the same time, TOHA requires significantly fewer extra computations.

Transfer results. The previous paragraph has shown that unsupervised methods, including the proposed TOHA, generally achieve significantly lower detection quality than supervised methods. However, it has previously been noted that supervised methods may experience considerable drops in quality when transferred to other datasets (Sky et al., 2024). So, we carried out the transferability experiments. Their results are presented in Table 3. We use the test parts of all datasets for method comparisons to prevent data leakage since the head selection for TOHA was performed on the training subset of RAGTruth QA. Here, we only provide the results for TOHA among all unsupervised methods, as the metrics in the unsupervised setting are duplicated from Table 1.

Table 1. ROC AUC (\uparrow) of hallucination detection techniques for three LLMs. The best results for each model are highlighted in **bold**, and the second best are underlined. The supervised and unsupervised methods are delimited by a horizontal line. TOP results for supervised methods are presented in **black**, while for unsupervised ones – in **green**.

Method	RAGTruth QA	RAGTruth Summ	RAGTruth Data2txt	CoQA
LLaMA-2-7B				
Attention-pooling probe	0.652	0.640	0.752	0.933
Linear probe	0.731	0.638	0.744	0.800
SelfCheckGPT	0.646	0.665	0.618	0.781
Semantic entropy	0.528	0.572	0.444	0.743
Tokenwise entropy	0.607	0.595	0.533	0.724
INSIDE	0.474	0.526	0.585	0.697
TOHA (ours)	0.646	0.638	0.573	0.858
LLaMA-2-13B				
Attention-pooling probe	0.768	0.573	0.573	0.936
Linear probe	0.705	0.472	0.589	0.696
SelfCheckGPT	0.675	0.508	0.559	0.867
Semantic entropy	0.581	0.536	0.359	0.831
Tokenwise entropy	0.626	0.588	0.514	0.659
INSIDE	0.557	0.569	0.511	0.518
TOHA (ours)	0.734	0.570	0.729	0.800
Mistral-7B				
Attention-pooling probe	0.791	0.661	0.685	0.978
Linear probe	0.841	0.714	0.69	0.922
SelfCheckGPT	0.709	0.600	0.63	0.941
Semantic entropy	0.543	0.558	0.431	0.861
Tokenwise entropy	0.701	0.598	0.445	0.759
INSIDE	0.652	0.558	0.427	0.766
TOHA (ours)	0.720	0.625	0.560	0.867

TOHA outperforms both supervised methods on almost all tasks, except for several cases where our method demonstrates second-best results. This observation aligns with our prior hypothesis. Unlike supervised methods, TOHA also demonstrates significantly better results than random for all the datasets and models.

What do hallucination patterns look like? As shown in Section 4, the topological divergences that we employ characterize the MSF that attaches the vertices R of the response to the vertices P of the prompt. For hallucination-aware heads, which consistently assign greater scores to hallucinated samples, we explored MSF patterns that are typical for hallucinated and grounded samples. The results for Mistral-7B are presented in Figure 5 (see Appendix D).

We identified two popular patterns among hallucinated samples: attention to the utility token $\langle s \rangle$ corresponding to the prompt beginning and “entanglement”. The former is an intuitive hallucination sign: instead of directing attention to meaningful parts of the context, the model focuses on a utility token. The “entanglement” — and, by the entanglement, we mean that many tokens seem to be linked to random

locations in the prompt — also allows intuitive explanation. When the attention scores of a token are distributed evenly across an entire text (which can be interpreted as a token’s uncertainty), many small weights in the attention matrix become associated with it, resulting in a greater MTop-Div value. This distribution of attention weights would entail that the edge in MSF connected to that token is equally likely to attach to any part of the query, creating the “entanglement”.

Inference time. We measure the inference time of the top-performing baselines and TOHA on the NVIDIA L40 GPU over 10 iterations with 3 *warmup*-iterations. In our experiments, we use 16 random samples from RAGTruth QA. For methods that require additional generations, we set $N = 20$, following the original papers (Manakul et al., 2024; Chen et al., 2024).

Table 4 indicates that supervised models are the most efficient, demonstrating two of the lowest inference times. In contrast, using SelfCheckGPT and semantic entropy is the most time-consuming. TOHA is significantly ahead of the top unsupervised methods in performance, being about 10

Table 2. ROC AUC (\uparrow) of hallucination detection techniques for LLaMA-3.1-8B. The supervised and unsupervised methods are delimited by a horizontal line. TOP results for supervised methods are presented in **black**, while for unsupervised ones – in **green**.

Method	SQuAD	CoQA
LLaMA-3.1-8B		
Attention-pooling probe	0.947	0.914
Linear probe	0.973	0.855
SelfCheckGPT	0.814	0.925
Semantic entropy	0.558	0.886
Tokenwise entropy	0.559	0.459
INSIDE	0.496	0.636
TOHA (ours)	0.883	0.703
Qwen2.5-7B		
Attention-pooling probe	0.850	0.661
Linear probe	0.808	0.695
SelfCheckGPT	0.642	0.769
Semantic entropy	0.688	0.742
Tokenwise entropy	0.477	0.640
INSIDE	0.582	0.566
TOHA (ours)	0.849	0.640

times faster than them.

6. Conclusion

This paper proposes TOHA (Algorithm 1) — a novel hallucination detection method based on the topological divergences of attention maps. In the core of TOHA lies our observation that specific attention heads demonstrate the same patterns in the presence of hallucinations, irrespective of the dataset. The hallucination scores obtained by TOHA are the average topological divergences from these heads. For these divergences, we prove several properties regarding their continuity and boundedness to ensure they can be considered reasonable hallucination scores. Extensive experiments have demonstrated that our method performs on par with or outperforms several state-of-the-art unsupervised baselines, including SelfCheckGPT (Manakul et al., 2024). Moreover, TOHA is significantly more computationally efficient than most, working an order of magnitude faster than SelfCheckGPT and semantic entropy. As for the supervised baselines, even though the proposed method does not reach their performance on the in-domain task, we showed that TOHA consistently outperforms them in the domain transfer setting. This capability of TOHA is of special importance for real-world applications, as user requests to LLMs may be much more diverse and complex than specific benchmarks. Thus, TOHA is a strong alternative to the existing methods.

Besides, we annotated two novel datasets containing hallucinated and grounded responses of several LLMs in the

Table 3. ROC AUC values for transfer of TOHA (unsupervised) and supervised methods’ comparison for three LLMs for subsets of RAGTruth QA, Summ, and Data2txt. TOP-1 results are highlighted with **bold font**, while TOP-2 are underlined.

Method		TOHA (ours)	Linear probe	Attn.-pool probe
Train	Test			
Mistral-7B				
QA	Summ	0.625	0.674	0.596
	Data2txt	0.56	0.548	0.468
Summ	QA	0.72	0.737	0.720
	Data2txt	0.56	<u>0.502</u>	<u>0.502</u>
Data2txt	QA	0.72	<u>0.618</u>	0.468
	Summ	0.625	0.348	<u>0.478</u>
LLaMA-2-7B				
QA	Summ	0.638	0.679	0.596
	Data2txt	0.573	0.496	0.520
Summ	QA	0.646	0.646	0.554
	Data2txt	0.573	<u>0.532</u>	0.476
Data2txt	QA	0.646	0.575	<u>0.601</u>
	Summ	0.638	0.665	0.590
LLaMA-2-13B				
QA	Summ	0.570	0.463	0.553
	Data2txt	0.729	0.633	<u>0.642</u>
Summ	QA	0.734	0.507	<u>0.563</u>
	Data2txt	0.729	0.502	<u>0.652</u>
Data2txt	QA	0.734	<u>0.479</u>	0.422
	Summ	0.570	<u>0.502</u>	0.456

Table 4. The comparison of methods’ inference time in milliseconds. The measurements were obtained using Mistral-7B. TOP-1 results are highlighted with **bold font**, while TOP-2 are underlined. The supervised and unsupervised methods are delimited by a horizontal line.

	Time, ms
Inference	$(0.68 \pm 0.11) \cdot 10^5$
Linear probe	0.16 \pm 0.02
Attention-pooling probe	<u>0.380 \pm 0.166</u>
SelfCheckGPT	$(1.46 \pm 0.06) \cdot 10^6$
Semantic entropy	$(1.45 \pm 0.06) \cdot 10^6$
Tokenwise entropy	(0.159 \pm 0.001) $\cdot 10^4$
TOHA	<u>$(1.82 \pm 0.18) \cdot 10^5$</u>

question-answering (QA) task. The obtained datasets will be released later to facilitate further research in the field. The code of the proposed method and the considered baselines will also be publicly available.

Impact statement. By introducing TOHA, we aim to address the following concerns:

- Recent breakthroughs in the NLP field are adopted ev-

everywhere, and the fear of missing out on new technology drives people without proper expertise to integrate LLMs in every possible aspect of their work. However, LLMs’ tendency for hallucinations is often neglected, which, in the best case, can incur financial losses and, in the worst — harm someone’s life (e.g., in domains such as healthcare and jurisprudence). Our work contributes towards the safe application of LLMs, thus facilitating broader adoption and integration of reliable AI technologies across various sectors.

- Transformer architecture is a core element of the most modern state-of-the-art NLP models. Our research offers deeper interpretability into how LLMs process information, shedding new light on the role of specific attention heads and their link to factual errors.
- Topological data analysis is usually seen as some kind of exotic. However, recent results show the effectiveness of TDA approaches, and therefore, we aim to shed more light on these methods in the hope that one day they will become a part of a researcher’s regular skill set.
- Despite the importance of hallucination detection, there exists a lack of annotated and validated datasets as well as pipelines for the generation of such datasets. With our work, several new datasets would make the problem more accessible and well-defined. Moreover, research would quickly produce new annotated datasets that would help to train and validate hallucination detection models.

References

- Azaria, A. and Mitchell, T. The internal state of an LLM knows when it’s lying. In Bouamor, H., Pino, J., and Bali, K. (eds.), *Findings of the Association for Computational Linguistics: EMNLP 2023*, pp. 967–976, Singapore, December 2023. Association for Computational Linguistics.
- Barannikov, S., Trofimov, I., Sotnikov, G., Trimbach, E., Korotin, A., Filippov, A., and Burnaev, E. Manifold topology divergence: a framework for comparing data manifolds. *Advances in neural information processing systems*, 34:7294–7305, 2021.
- Barannikov, S. A. The framed Morse complex and its invariants, December 1994. ISSN 2472-4912.
- Bavaresco, A., Bernardi, R., Bertolazzi, L., Elliott, D., Fernández, R., Gatt, A., Ghaleb, E., Giulianelli, M., Hanna, M., Koller, A., Martins, A. F. T., Mondorf, P., Neplenbroek, V., Pezzelle, S., Plank, B., Schlangen, D., Suglia, A., Surikuchi, A. K., Takmaz, E., and Testoni, A. LLMs instead of human judges? A large scale empirical study across 20 NLP evaluation tasks. *CoRR*, abs/2406.18403, 2024.
- Brown, T., Mann, B., Ryder, N., Subbiah, M., Kaplan, J. D., Dhariwal, P., Neelakantan, A., Shyam, P., Sastry, G., Askell, A., et al. Language models are few-shot learners. *Advances in neural information processing systems*, 33: 1877–1901, 2020.
- Chazal, F. and Michel, B. An introduction to topological data analysis: Fundamental and practical aspects for data scientists. *Frontiers in Artificial Intelligence*, 4, 2017.
- Chen, C., Liu, K., Chen, Z., Gu, Y., Wu, Y., Tao, M., Fu, Z., and Ye, J. INSIDE: LLMs’ internal states retain the power of hallucination detection. In *The Twelfth International Conference on Learning Representations*, 2024.
- Cherniavskii, D., Tulchinskii, E., Mikhailov, V., Proskurina, I., Kushnareva, L., Artemova, E., Barannikov, S., Piontkovskaya, I., Piontkovski, D., and Burnaev, E. Acceptability judgements via examining the topology of attention maps. In Goldberg, Y., Kozareva, Z., and Zhang, Y. (eds.), *Findings of the Association for Computational Linguistics: EMNLP 2022*, pp. 88–107, Abu Dhabi, United Arab Emirates, December 2022. Association for Computational Linguistics.
- Chkribene, Z., Hamila, R., Gouissem, A., and Devrim, U. Large language models (LLM) in industry: A survey of applications, challenges, and trends. In *2024 IEEE 21st International Conference on Smart Communities: Improving Quality of Life using AI, Robotics and IoT (HONET)*, pp. 229–234. IEEE, 2024.
- Chuang, Y.-S., Qiu, L., Hsieh, C.-Y., Krishna, R., Kim, Y., and Glass, J. Lookback lens: Detecting and mitigating contextual hallucinations in large language models using only attention maps. In *Proceedings of the 2024 Conference on Empirical Methods in Natural Language Processing*, pp. 1419–1436, 2024.
- Fadeeva, E., Rubashevskii, A., Shelmanov, A., Petrakov, S., Li, H., Mubarak, H., Tsymbalov, E., Kuzmin, G., Panchenko, A., Baldwin, T., et al. Fact-checking the output of large language models via token-level uncertainty quantification. *arXiv preprint arXiv:2403.04696*, 2024.
- Farquhar, S., Kossen, J., Kuhn, L., and Gal, Y. Detecting hallucinations in large language models using semantic entropy. *Nature*, 630(8017):625–630, 2024.
- Gao, Y., Xiong, Y., Gao, X., Jia, K., Pan, J., Bi, Y., Dai, Y., Sun, J., and Wang, H. Retrieval-augmented generation for large language models: A survey. *arXiv preprint arXiv:2312.10997*, 2023.

- Gould, R., Ong, E., Ogden, G., and Conmy, A. Successor heads: Recurring, interpretable attention heads in the wild. In *The Twelfth International Conference on Learning Representations*, 2024.
- Han, J., Kossen, J., Razzak, M., Schut, L., Malik, S. A., and Gal, Y. Semantic entropy probes: Robust and cheap hallucination detection in LLMs. In *ICML 2024 Workshop on Foundation Models in the Wild*, 2024.
- Hensel, F., Moor, M., and Rieck, B. A survey of topological machine learning methods. *Frontiers in Artificial Intelligence*, 4:681108, 2021.
- Huang, L., Yu, W., Ma, W., Zhong, W., Feng, Z., Wang, H., Chen, Q., Peng, W., Feng, X., Qin, B., et al. A survey on hallucination in large language models: Principles, taxonomy, challenges, and open questions. *ACM Transactions on Information Systems*, 2023.
- Hurst, A., Lerer, A., Goucher, A. P., Perelman, A., Ramesh, A., Clark, A., Ostrow, A., Welihinda, A., Hayes, A., Radford, A., et al. GPT-4o system card. *arXiv preprint arXiv:2410.21276*, 2024.
- Jiang, A. Q., Sablayrolles, A., Mensch, A., Bamford, C., Chaplot, D. S., Casas, D. d. l., Bressand, F., Lengyel, G., Lample, G., Saulnier, L., et al. Mistral 7b. *arXiv preprint arXiv:2310.06825*, 2023.
- Kadavath, S., Conerly, T., Askell, A., Henighan, T., Drain, D., Perez, E., Schiefer, N., Hatfield-Dodds, Z., DasSarma, N., Tran-Johnson, E., et al. Language models (mostly) know what they know. *arXiv preprint arXiv:2207.05221*, 2022.
- Kostenok, E., Cherniavskii, D., and Zaytsev, A. Uncertainty estimation of transformers’ predictions via topological analysis of the attention matrices. *arXiv preprint arXiv:2308.11295*, 2023.
- Kuhn, L., Gal, Y., and Farquhar, S. Semantic uncertainty: Linguistic invariances for uncertainty estimation in natural language generation. In *The Eleventh International Conference on Learning Representations*, 2023.
- Kushnareva, L., Cherniavskii, D., Mikhailov, V., Artemova, E., Barannikov, S., Bernstein, A., Piontkovskaya, I., Piontkovski, D., and Burnaev, E. Artificial text detection via examining the topology of attention maps. In *Proceedings of the 2021 Conference on Empirical Methods in Natural Language Processing*, pp. 635–649, 2021.
- Lebret, R., Grangier, D., and Auli, M. Neural text generation from structured data with application to the biography domain. In *Proceedings of the 2016 Conference on Empirical Methods in Natural Language Processing*, pp. 1203–1213, 2016.
- Lin, S., Hilton, J., and Evans, O. TruthfulQA: Measuring how models mimic human falsehoods. In *Proceedings of the 60th Annual Meeting of the Association for Computational Linguistics (Volume 1: Long Papers)*, pp. 3214–3252, 2022.
- Lin, Z., Trivedi, S., and Sun, J. Generating with confidence: Uncertainty quantification for black-box large language models. *Transactions on Machine Learning Research*, 2024. ISSN 2835-8856.
- Manakul, P., Liusie, A., and Gales, M. SelfCheckGPT: Zero-resource black-box hallucination detection for generative large language models. In *The 2023 Conference on Empirical Methods in Natural Language Processing*, 2024.
- Min, S., Krishna, K., Lyu, X., Lewis, M., Yih, W.-t., Koh, P., Iyyer, M., Zettlemoyer, L., and Hajishirzi, H. Factscore: Fine-grained atomic evaluation of factual precision in long form text generation. In *Proceedings of the 2023 Conference on Empirical Methods in Natural Language Processing*, pp. 12076–12100, 2023.
- Narayan, S., Cohen, S., and Lapata, M. Don’t give me the details, just the summary! Topic-aware convolutional neural networks for extreme summarization. In *2018 Conference on Empirical Methods in Natural Language Processing*, pp. 1797–1807. Association for Computational Linguistics, 2018.
- Niu, C., Wu, Y., Zhu, J., Xu, S., Shum, K., Zhong, R., Song, J., and Zhang, T. RAGTruth: A hallucination corpus for developing trustworthy retrieval-augmented language models. *arXiv preprint arXiv:2401.00396*, 2023.
- Proskurina, I., Artemova, E., and Piontkovskaya, I. Can BERT eat RuCoLA? Topological data analysis to explain. In *Proceedings of the 9th Workshop on Slavic Natural Language Processing 2023 (SlavicNLP 2023)*, May 2023a.
- Proskurina, I., Artemova, E., and Piontkovskaya, I. Can bert eat rucola? topological data analysis to explain. In *Proceedings of the 9th Workshop on Slavic Natural Language Processing 2023 (SlavicNLP 2023)*, pp. 123–137, 2023b.
- Rajpurkar, P., Zhang, J., Lopyrev, K., and Liang, P. SQuAD: 100,000+ questions for machine comprehension of text. In Su, J., Duh, K., and Carreras, X. (eds.), *Proceedings of the 2016 Conference on Empirical Methods in Natural Language Processing*, 2016.
- Reddy, S., Chen, D., and Manning, C. D. CoQA: A conversational question answering challenge. *Transactions of the Association for Computational Linguistics*, 7:249–266, 2019.

- Sky, C.-W., Van Durme, B., Eisner, J., and Kedzie, C. Do androids know they’re only dreaming of electric sheep? In *Findings of the Association for Computational Linguistics ACL 2024*, pp. 4401–4420, 2024.
- Touvron, H., Lavril, T., Izacard, G., Martinet, X., Lachaux, M.-A., Lacroix, T., Rozière, B., Goyal, N., Hambro, E., Azhar, F., et al. Llama: Open and efficient foundation language models. *arXiv preprint arXiv:2302.13971*, 2023.
- Tulchinskii, E., Kuznetsov, K., Cherniavskii, D., Barannikov, S., Nikolenko, S., and Burnaev, E. Topological data analysis for speech processing. In *Proceedings of the Annual Conference of the International Speech Communication Association, INTERSPEECH*, pp. 311–315, 2023.
- Tulchinskii, E., Kuznetsov, K., Kushnareva, L., Cherniavskii, D., Nikolenko, S., Burnaev, E., Barannikov, S., and Piontkovskaya, I. Intrinsic dimension estimation for robust detection of ai-generated texts. *Advances in Neural Information Processing Systems*, 36, 2024.
- Uchendu, A. and Le, T. Unveiling topological structures in text: A comprehensive survey of topological data analysis applications in NLP. *arXiv preprint arXiv:2411.10298*, 2024.
- Vakhrushev, A., Ryzhkov, A., Savchenko, M., Simakov, D., Damdinov, R., and Tuzhilin, A. LightAutoML: AutoML solution for a large financial services ecosystem. *arXiv preprint arXiv:2109.01528*, 2021.
- Vaswani, A., Shazeer, N., Parmar, N., Uszkoreit, J., Jones, L., Gomez, A., Kaiser, L., and Polosukhin, I. Attention is all you need. In *Advances in Neural Information Processing Systems*, 2017.
- Voita, E., Talbot, D., Moiseev, F., Sennrich, R., and Titov, I. Analyzing multi-head self-attention: Specialized heads do the heavy lifting, the rest can be pruned. In *Proceedings of the 57th Annual Meeting of the Association for Computational Linguistics*, pp. 5797–5808, 2019.
- Wang, Y., Wang, M., Manzoor, M. A., Liu, F., Georgiev, G., Das, R., and Nakov, P. Factuality of large language models: A survey. In *Proceedings of the 2024 Conference on Empirical Methods in Natural Language Processing*, pp. 19519–19529, 2024.
- Xiong, M., Hu, Z., Lu, X., LI, Y., Fu, J., He, J., and Hooi, B. Can LLMs express their uncertainty? an empirical evaluation of confidence elicitation in LLMs. In *The Twelfth International Conference on Learning Representations*, 2024.
- Zhang, Y., Li, Y., Cui, L., Cai, D., Liu, L., Fu, T., Huang, X., Zhao, E., Zhang, Y., Chen, Y., et al. Siren’s song in the AI ocean: a survey on hallucination in large language models. *arXiv preprint arXiv:2309.01219*, 2023.
- Zhao, Y., Zhang, J., Chern, I., Gao, S., Liu, P., He, J., et al. Felm: Benchmarking factuality evaluation of large language models. *Advances in Neural Information Processing Systems*, 36:44502–44523, 2023.

A. Topological data analysis: background

A simplicial complex S is a collection of simplices such that every face of a simplex $\sigma \in S$ is also in S . Simplices are the higher-dimensional generalizations of triangles; a 0-simplex is a vertex, a 1-simplex is an edge, a 2-simplex is a triangle, and so forth. Formally, given a finite set X , an n -simplex σ is an $(n + 1)$ subset of X . Simplicial complexes are fundamental objects in algebraic and combinatorial topology, serving as a discrete analog to topological spaces.

The Vietoris-Rips complex $VR_\varepsilon(X)$ of a weighted graph $G = (V_G, E_G)$ with distance threshold $\varepsilon > 0$ is defined as follows:

$$VR_\varepsilon(G) = \left\{ \sigma \subseteq V_G \mid \forall v_i, v_j \in \sigma, w(e_{ij}) \leq \varepsilon \right\},$$

where w is the edge weight function associated with G .

Homology groups H_k are invariants used in algebraic topology to study the topological properties of a space. Let $C_k(S)$ denote vector space over $\mathbb{Z}/2\mathbb{Z}$, with the basis consisting of k -dimensional simplices of S . Elements of C_k are called chains. Formally, homology groups are derived from a chain complex $(C_\bullet, \partial_\bullet)$, which is a sequence of C_k connected by boundary maps ∂_k :

$$C_\bullet : \cdots \rightarrow C_{k+1} \xrightarrow{\partial_{k+1}} C_k \xrightarrow{\partial_k} \cdots, \quad \partial_k \circ \partial_{k+1} = 0.$$

The k -th homology group H_k is defined as the quotient of the group of k -cycles (chains whose boundary is zero) by the group of k -boundaries (chains that are the boundary of a $(k + 1)$ -chain). Mathematically, this is expressed as:

$$H_k(S) = Z_k(S) / B_k(S),$$

where $Z_k = \ker \partial_k = \{c \in C_k \mid \partial_k(c) = 0\}$ and $B_k = \text{im } \partial_{k+1} = \{\partial_{k+1}(c) \mid c \in C_{k+1}\}$ is the group of k -boundaries. The elements of $H_k(S)$ represent various k -dimensional topological features in S . Elements of a basis in $H_k(S)$ correspond to a set of basic topological features.

A filtration of simplicial complexes \mathcal{F} is a family of nested simplicial complexes:

$$\mathcal{F} : \emptyset \subseteq S_1 \subseteq S_2 \subseteq \cdots \subseteq S_n = S,$$

where each S_k is a simplicial complex itself. In practice, the filtrations of simplicial complexes are usually obtained for sequences of increasing thresholds $0 < \varepsilon_1 < \cdots < \varepsilon_n$. For example, simplicial complexes $VR_{\varepsilon_i}(X)$ form a filtration

$$\mathcal{F}_{VR}(X) : \emptyset \subseteq VR_{\varepsilon_1}(X) \subseteq VR_{\varepsilon_2}(X) \subseteq \cdots \subseteq VR_{\varepsilon_n}(X) = VR(X)$$

As a threshold ε increases, new topological features (e.g., connected components, holes) can appear and disappear. The persistent homology tool is used to track the dynamics of these topological features. Formally, the k -th persistent homology of S is the pair of sets of vector spaces $\{H_k(S_i) \mid 0 \leq i \leq n\}$ and maps f_{ij} , where $f_{ij} : H_k(S_i) \rightarrow H_k(S_j)$ is a map induced by the embedding $S_i \subseteq S_j$. Each persistent homology class in this sequence is “born” at some S_i and “dies” at some S_j or never dies (Barannikov, 1994). This birth-death process of a basic set of independent topological features can be visualized as the set of intervals $[\varepsilon_{\text{birth}}, \varepsilon_{\text{death}}]$ called barcode (see Figure 4). The features with 0 lifespans are typically excluded. The horizontal axis is a sequence of thresholds ε , and each horizontal bar corresponds to a single feature. We begin with $|X| = m$ connected components (all of them are “born”), and as ε increases, their pairs are merged (each merge corresponds to a “death” of a feature). The 0-th barcode construction procedure is equivalent to Kruskal’s algorithm for minimum spanning tree (MST), the bars in the barcode correspond to the edges in the MST of X (Tulchinskii et al., 2023).

B. MTop-Div on graphs properties

Proof of Proposition 4.1.

1. The 0-th Cross-Barcode coincides with the set of edges in the minimal spanning tree of the weighted graph G with all the weights within P vertex subset equal zero. Excluding the zero weight edges, this edge set coincides with the minimal spanning forest attaching the vertex set R to P vertices.

Proof of Proposition 4.2.

1. Denote by $\text{MSF}(R, P)$ the minimum spanning forest attaching R to P . Note that we have properties 4.1, so

$$\text{MTop-Div}(R, P) = \sum_{e \in \text{MSF}(R, P)} w(e). \quad (7)$$

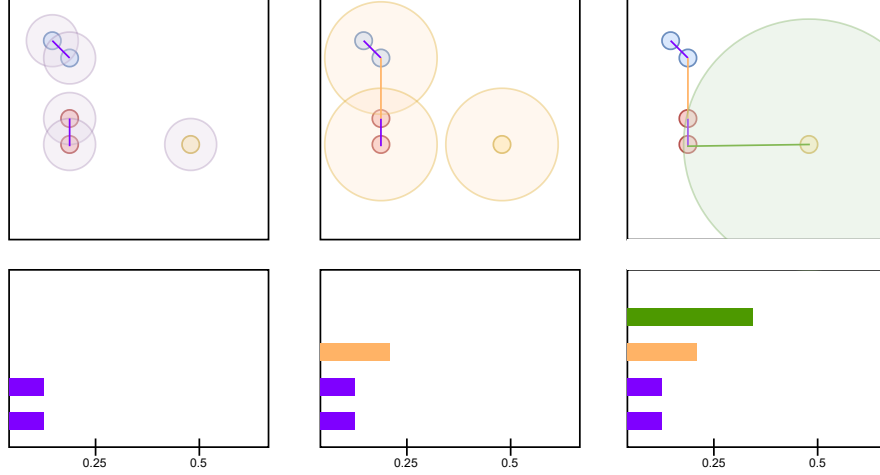


Figure 4. H_0 barcode construction. As the threshold increases, the separate connected components merge, resulting in the death of topological features. The horizontal axis is a sequence of thresholds ε , and each horizontal bar corresponds to a single feature.

Therefore, we have to show that the weight of $\text{MSF}(R, P)$ does not change significantly when all weights are changed by no more than ε .

There are two possibilities: 1) after a change, all MSF edges remain the same, or 2) some edges are replaced with other edges. In the first case, it is obvious that the total sum of edges weights changes by no more than $\delta = \varepsilon \cdot \#\text{edges}(\text{MSF}(R, P)) = \varepsilon \cdot |R|$. Consider the second case. Denote by MSF_{prev} the original MSF, by MSF_{new} — the MSF after the change; let w be the edge weight function before the change, \hat{w} — after the change. The following inequalities hold:

$$\hat{w}(\text{MSF}_{\text{new}}) < \hat{w}(\text{MSF}_{\text{prev}}); \quad (8)$$

$$w(\text{MSF}_{\text{prev}}) - \delta \leq \hat{w}(\text{MSF}_{\text{prev}}) \leq w(\text{MSF}_{\text{prev}}) + \delta; \quad (9)$$

$$w(\text{MSF}_{\text{new}}) - \delta \leq \hat{w}(\text{MSF}_{\text{new}}) \leq w(\text{MSF}_{\text{new}}) + \delta; \quad (10)$$

$$w(\text{MSF}_{\text{new}}) \geq w(\text{MSF}_{\text{prev}}). \quad (11)$$

From (8)-(9) follows that $\hat{w}(\text{MSF}_{\text{new}}) < w(\text{MSF}_{\text{prev}}) + \delta$; from (10)-(11) follows that $\hat{w}(\text{MSF}_{\text{new}}) \geq w(\text{MSF}_{\text{prev}}) - \delta$, QED.

2. We have to check the definition of the exact sequence: $\text{Ker}(r_i) = \text{Im}(r_{i+1})$. For a pair r_0, r_1 , it is equivalent to the surjectivity of r_1 . The H_0 homology group of a graph corresponds to the connected components of the graph. The set of edges $E_{(G,w)}^{\leq \alpha} = \{e \in E_G | w_e \leq \alpha\}$ is always a subset in the analogous set of the weighted graph $(G, w_{(R \cup P)/P})$ with all weight edges between P vertices set to zero. Therefore, the map r_1 between their connected components is surjective. Similarly the kernel of the map r_1 is spanned by the differences of two connected components, that are merged after adding some of the edges between P vertices, and any such difference lies in the image of the map r_2 . Also any two vertices from P belong to the same connected component in the graph $(G, w_{(R \cup P)/P} \leq \alpha)$, hence the image of r_2 is in the kernel of r_1 .

Therefore, the considered sequence is exact indeed.

C. Datasets

SQuAD (Rajpurkar et al., 2016) and CoQA (Reddy et al., 2019) are question-answering benchmarks previously used as a basis for collecting hallucination detection datasets (Kuhn et al., 2023; Manakul et al., 2024). However, these datasets have not been published before, complicating further up-to-date research.

We have annotated the responses of several LLMs to the questions from SQuAD and CoQA using GPT-4o in an automated regime. We will release these datasets publicly. Here, we provide the methodology for the automated annotation and evaluate its quality, motivating the usage of the introduced datasets in practice.

SQuAD	CoQA
Given the context, answer the question in a brief but complete sentence. Note that your answer should be strictly based on the given context. In case the context does not contain the necessary information to answer the question, please reply with "Unable to answer based on given context". <i>Context:</i> Once upon a time, in a quiet village, there lived a kind old baker named Henry. He was known for his delicious bread and warm smile. One day, a traveler arrived, tired and hungry, and Henry welcomed him with a fresh loaf. <i>Question:</i> Who was known for baking delicious bread? <i>Answer:</i>	Once upon a time, in a quiet village, there lived a kind old baker named Henry. He was known for his delicious bread and warm smile. One day, a traveler arrived, tired and hungry, Henry welcomed him with a fresh loaf. <i>Q:</i> What was Henry known for? <i>A:</i> Baking delicious bread. <i>Q:</i> What else? <i>A:</i> Warm smile. <i>Q:</i> How did the traveler feel when he arrived? <i>A:</i> Tired and hungry. <i>Q:</i> What did Henry give the traveler?

Table 5. Examples of prompts used during generation for CoQA and SQuAD (we add additional delimiter spaces and formatting that are non-present in actual prompts for better readability). SQuAD contains instructions followed by context and questions. In CoQA, the prompt has only a contextual passage followed by a questions-answers series, with the last question being the actual one.

You are an AI assistant specialized in detecting hallucinations in question-answering tasks. Your job is to analyze the given context, question, and generated answer to identify whether the answer contains any hallucinations. Examples:

Example 1.
Context:
The city of Paris is the capital of France. It is known for its iconic landmarks like the Eiffel Tower and Notre Dame Cathedral.
The city is situated in the northern part of the country, near the Seine River.
Question: Is Paris the capital of Germany?
Generated answer: Yes, Paris is the capital of Germany.
Hallucination: Yes.

Example 2.
Context:
The city of Paris is the capital of France.
It is known for its iconic landmarks like the Eiffel Tower and Notre Dame Cathedral.
The city is situated in the northern part of the country, near the Seine River.
Question: Is Paris the capital of Germany?
Generated answer: No, Paris is not the capital of Germany. According to the context, Paris is the capital of France.
Hallucination: No.

You should determine if the answer contains hallucinations according to the hallucination types above. If you cannot decide if the generated answer is a hallucination, write "N/A." as the answer. The answer you give MUST be ONLY "Yes.", "No." or "N/A."; do NOT give ANY explanation.

Table 6. Example of annotation prompt passed to GPT-4o (we add additional delimiter spaces and formatting non-present in actual prompts for better readability).

Prompt number		1	2	3	4	5
CoQA	Accuracy (\uparrow)	0.809 \pm 0.017	0.861 \pm 0.015	0.742 \pm 0.003	0.795 \pm 0.009	0.831 \pm 0.025
	Precision (\uparrow)	0.849 \pm 0.021	0.911 \pm 0.007	0.771 \pm 0.003	0.828 \pm 0.011	0.860 \pm 0.012
	Recall (\uparrow)	0.871 \pm 0.004	0.877 \pm 0.019	0.877 \pm 0.013	0.877 \pm 0.005	0.893 \pm 0.027
SQuAD	Accuracy (\uparrow)	0.831 \pm 0.003	0.857 \pm 0.018	0.857 \pm 0.008	0.872 \pm 0.003	0.854 \pm 0.007
	Precision (\uparrow)	0.813 \pm 0.002	0.831 \pm 0.028	0.845 \pm 0.021	0.850 \pm 0.011	0.847 \pm 0.007
	Recall (\uparrow)	0.796 \pm 0.008	0.839 \pm 0.010	0.823 \pm 0.023	0.858 \pm 0.018	0.813 \pm 0.017

Average	Accuracy (\uparrow)	Precision (\uparrow)	Recall (\uparrow)
CoQA	0.808	0.844	0.879
SQuAD	0.854	0.837	0.826

Table 7. Classification metrics of GPT-4o annotation for CoQA and SQuAD with human labels considered actual annotation. The top table shows metric scores for different variants of prompts used. The bottom table shows the metric scores averaged across all prompt variants.

C.1. Data Generation & Annotation

Generation. We generate responses from a language model (LLM) for the CoQA and SQuAD datasets, employing different prompting strategies for each dataset while keeping these strategies consistent across models (see prompt examples in Table 5). For SQuAD, responses are generated using a zero-shot approach. In contrast, for CoQA, we create queries in a few-shot manner without providing specific instructions, following (Lin et al., 2024): each sample consists of a passage and a series of question-answer pairs, concluding with a final question that the model is expected to answer.

Annotation: automated vs human. We treat hallucination detection as a binary classification problem; our target indicates whether a hallucination is present anywhere in the model’s response. Two approaches to annotating model generations were considered: 1) automated annotation using an LLM (in our case, GPT-4o), and 2) manual annotation by human experts.

During the automated annotation process, we provide an LLM’s output preceded by an instruction (prompt) to GPT-4o. In this prompt, GPT-4o is asked to determine whether the output contains hallucinations, and we expect a single-word response of either “Yes” or “No.” An example of such an instruction is shown in Table 6.

For human annotation, we asked three team members with at least upper-intermediate English proficiency to independently annotate approximately 100 samples from each dataset. We selected samples where all annotators reached a consensus and considered these annotations the ground truth hallucination labels.

To further evaluate GPT-4o, we conducted automatic annotation using several variations of prompts, each reformulating the task for GPT-4o, including zero-shot and few-shot versions. We then compared these annotations to the actual hallucination labels. The results, presented in Table 7, demonstrate a consistent alignment between GPT-4o’s annotations and those made by humans, regardless of the specific prompt. This consistency confirms the robustness of our approach to the exact form of instruction.

Based on these findings, we prefer automated annotation as a cost-effective and efficient alternative to human experts.

Annotation: general pipeline. CoQA and SQuAD contain questions and the ground truth answers to those questions. We employed them to reduce the potential false positive labels in the following way: 1) we compute Rouge-L scores between ground truth answers and the model’s response, and 2) check if any of the grounded answers are a substring of the response. The responses corresponding to Rouge-L = 1 are immediately labeled as grounded (complete match). The responses that meet the following conditions: 1) corresponding Rouge-L ≤ 0.3 (as in (Kuhn et al., 2023)), and 2) none of the ground truth answers is its’ sub-string, are labeled as potential hallucinations and are then annotated via GPT-4o. The responses that are confirmed to be hallucinated by GPT-4o are finally annotated as hallucinations.

Detailed statistics for each dataset can be seen in Table 8. The number of samples in the datasets varies across models, as we tried to maintain a balance of hallucinated and grounded responses, as well as to ensure sample cleanness and minimize mislabeling. The procedure outlined above selects a different number of objects in a sample depending on the quality of the model’s responses.

Model	CoQA		SQuAD	
	Hal.	Grounded	Hal.	Grounded
Mistral-7B	776	776	✗	✗
LLaMA-2-7B	375	375	✗	✗
LLaMA-2-13B	279	384	✗	✗
LLaMA-3.1-8B	190	247	350	400
Qwen2.5-7B	124	183	215	249

Table 8. Datasets statistics. Number of hallucinated and grounded samples of each model.

D. Other experiment results

D.1. Hallucination patterns

Due to a lack of space in the paper’s main section, we illustrate typical patterns within hallucination-aware heads. Pictures a) and c) display the minimal spanning forest (MSF) of a hallucinated example, while b) and d) — the MSF of a grounded one. For this illustration, we used two examples from the RAGTruth QA dataset corresponding to the extreme MTop-Div values

for the (19, 4) head of Mistral-7B. The layout is similar to the one in Figure 2: on the left side, we arrange prompt tokens in the same order as they are present in the text, while the response tokens are located on the right. Blue color denotes the tokens of the instruction (“Briefly answer the following...”), red color — tokens of the context, green color — grounded tokens of the response, yellow color — the hallucinated tokens of the response. Here, the “entanglement” and the attention to the utility token $\langle s \rangle$ patterns are apparent.

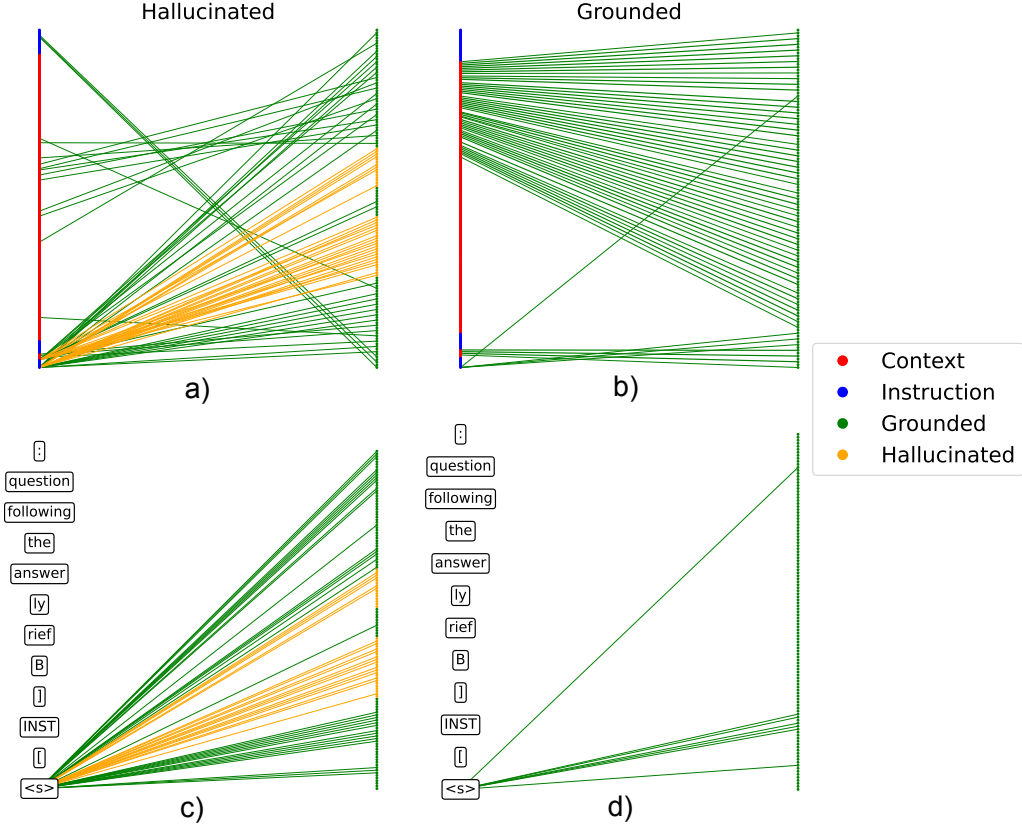


Figure 5. Typical patterns within the hallucination aware-heads. Two samples from RAGTruth QA are shown. Figures a) and c) correspond to the hallucinated sample with large MTop-Div value, while b) and d) — to the grounded one, with a small one. Model: Mistral-7B.

D.2. Transfer within QA datasets

We carried out additional transferability experiments for all our models among QA datasets. For LLaMA-2-7B, Mistral-7B, and LLaMA-2-13b, we considered transfer between the RAGTruth QA and CoQA datasets, while for Qwen2.5-7B and LLaMA-3.1-8B — between SQuAD and CoQA. The results are provided in Table 9. TOHA mostly outperforms supervised methods, which aligns well with the transferability experiments in section 5.

D.3. Classifier on topological features

Our preliminary experiments on developing the TDA-based hallucination detector included training classifiers on the topological features previously used for other NLP tasks (Kushnareva et al., 2021; Cherniavskii et al., 2022). We considered features extracted from barcodes (i.e., the sum of lengths of bars) and “naive” topological features (i.e., average vertex degree) of attention graphs. As we considered supervised methods, our primary goal was to determine whether these features can enhance the performance of simple hidden states-based classifiers. To make the most of the considered features and their aggregations, we trained an AutoML model (Vakhrushev et al., 2021) on different feature sets — only hidden states; only barcode features; hidden states and barcode features; hidden states, barcode features and “naive” topological features. The results are presented in Table 10.

Table 9. ROC AUC values for transfer of TOHA (unsupervised) and supervised methods’ comparison for five LLMs for question answering datasets. TOP-1 results are highlighted with **bold font**, while TOP-2 are underlined.

Method		TOHA (ours)	Linear probe	Attn.-pool probe
Train	Test			
Mistral-7B				
RAGTruth	CoQA	0.867	0.635	<u>0.687</u>
CoQA	RAGTruth	0.720	0.596	<u>0.611</u>
LLaMA-2-7B				
RAGTruth	CoQA	0.858	<u>0.628</u>	0.623
CoQA	RAGTruth	0.646	<u>0.497</u>	<u>0.532</u>
LLaMA-2-13B				
RAGTruth	CoQA	0.800	0.574	<u>0.617</u>
CoQA	RAGTruth	0.734	<u>0.553</u>	0.52
LLaMA-3.1-8B				
SQuAD	CoQA	0.703	<u>0.733</u>	0.761
CoQA	SQuAD	0.883	<u>0.730</u>	0.582
Qwen2.5-7B				
SQuAD	CoQA	0.640	0.522	<u>0.562</u>
CoQA	SQuAD	0.849	0.510	<u>0.553</u>

As we can see, a classifier on the proposed features alone does not achieve the performance of a hidden states-based classifier. When concatenated to hidden states, they do not provide significant metric gains. Our conclusion was straightforward: we needed to develop other approaches to this problem.

We also considered training classifiers on the concatenated MTop-Div values from all layers and heads of the models, along with classifiers on top of the concatenated MTop-Div values and hidden states. These results are also displayed in Table 10. We can see that models employing MTop-Div outperform pure hidden states-based classifiers. However, calculating MTop-Div vales from all heads and layers is very computationally expensive, therefore, this method is not very practical. The most valuable conclusion that can be made from this comparison is that the MTop-Div values are more informative from the hallucination detection point of view than both standard TDA features and hidden states of a model.

Table 10. Performance of supervised classifiers on top of various feature combinations. ROC-AUC values are presented. “Hiddens” refer to hidden states of a model. TOP-1 results are highlighted with **bold font**, while TOP-2 are underlined.

Method	RAGTruth QA	CoQA
Mistral-7B		
Linear probe	0.841	0.922
Classifier on MTop-Div	0.858	<u>0.972</u>
Topological features	0.671	0.694
Hiddens + top. features	<u>0.850</u>	0.923
Hiddens + MTop-Div	<u>0.837</u>	0.978
LLaMA-2-7B		
Linear probe	0.731	0.800
Classifier on MTop-Div	0.750	0.960
Topological features	0.689	0.699
Hiddens + top. features	<u>0.744</u>	0.863
Hiddens + MTop-Div	0.721	<u>0.950</u>

E. Implementation details

In this section, we provide the main choices of parameters for baselines.

- For methods that rely on hidden states, we considered the outputs from the 16th layer, as the ablation studies in (Sky et al., 2024; Azaria & Mitchell, 2023) showed that middle layers contain the maximum amount of information in the context of factuality evaluation.
- In the linear probing method and INSIDE, we used the last token representation as an embedding of an entire sentence, following the ablation study in (Chen et al., 2024).
- For methods relying on multiple generations, we used 20 additional generations based on the results of (Manakul et al., 2024; Chen et al., 2024).
- As for an aggregation of token entropies from the entire sequence, we chose the maximum value to be the score for tokenwise entropy as our own results and the results from (Manakul et al., 2024) showed that it demonstrates better performance than simple averaging.

Our repository is available at <https://anonymous.4open.science/r/tda4hallu-0679>.